Chapter 8
Identification in Closed-Loop Operation

8.1 Introduction

There are two reasons for considering identification in closed-loop operation in the context of active vibration control systems:

- obtaining improved system models for controller redesign; and
- retuning of the controller without opening the loop.

The objective of identification in closed-loop is to obtain a plant model describing as precisely as possible the behaviour of the real closed-loop system for a given controller. In other words, the objective of system identification in closed-loop is to search for a plant model that in feedback with the controller operating on the true plant will lead to a closed-loop transfer function (sensitivity function) that is as close as possible to that of the real closed-loop system. If the performance of the closed-loop system is not satisfactory, it is expected that this model identified in closed-loop will allow the redesign of the controller in order to improve the performance of the real-time control system.

It has been shown in [1, 2], as well as in many other references, that identification in closed-loop, provided that appropriate identification algorithms are used, leads in general to better models for controller design.

In order to understand the potential of the identification in closed-loop as well as the difficulties which can be encountered, let us consider the case of the plant model identification in closed-loop where the external excitation is added to the controller output (see Fig. 8.1a). Figure 8.1b shows an equivalent scheme that emphasizes the transfer function between the external excitation r_u and the plant input u, as well as the effect of the measurement noise upon the plant input. Assume that the external excitation is a PRBS that has almost constant frequency spectrum from 0 to $0.5f_s$.

One observes that the effective plant input corresponds to the external excitation filtered by the output sensitivity function S_{yp} (see Sect. 7.1), whose magnitude has a maximum in the frequency regions close to the critical point $[-1, j0]$ (see Sect. 7.2.4). Therefore the frequency spectrum of the effective input applied to the

© Springer International Publishing Switzerland 2017

I.D. Landau et al., *Adaptive and Robust Active Vibration Control*,
Advances in Industrial Control, DOI 10.1007/978-3-319-41450-8_8

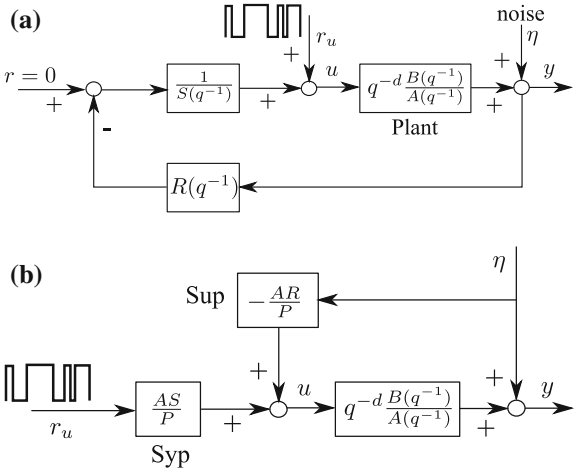

Fig. 8.1 Identification in closed-loop: **a** excitation added to the control output, **b** equivalent representation

plant will be enhanced in these frequency regions. As a consequence, the quality of the identified model in these critical regions for stability and performance will be improved. Unfortunately, in the meantime, the feedback introduces a correlation between the measurement noise and the plant input. This leads to an important bias on the estimated parameters if one would like to identify the plant model with open-loop techniques.

Therefore, for a good identification in closed-loop operation one needs identification methods *that take advantage of the "improved" characteristics of the effective excitation signal applied to the plant input but which are not affected by the noise in the context of feedback*. An efficient solution for this problem is provided by the "closed-loop output error" method (CLOE) that will be presented next.

8.2 Closed-Loop Output Error Identification Methods

The Principle

The principle of closed-loop output error identification algorithms is illustrated in Fig. 8.2. The upper part represents the true closed-loop system and the lower part represents an adjustable predictor of the closed-loop. This closed-loop predictor uses a controller identical to the one used on the real-time system.

The prediction error between the output of the real-time closed-loop system and the closed-loop predictor (closed-loop output error) is a measure of the difference between the true plant model and the estimated one. This error can be used to adapt the estimated plant model such that the closed-loop prediction error is minimized (in the sense of a certain criterion). In other words, the objective of the identification

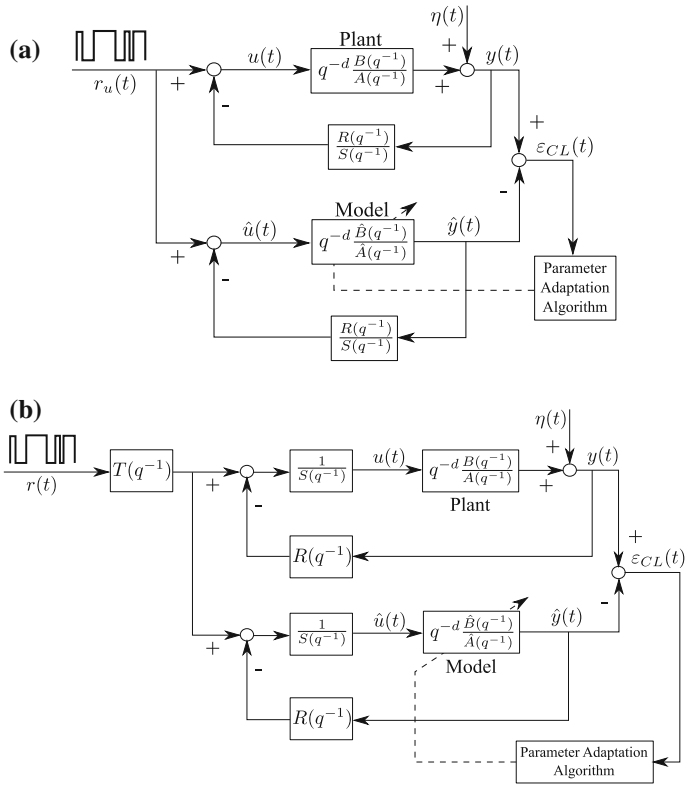

Fig. 8.2 Closed-loop output error identification method. **a** Excitation superposed to control output. **b** Excitation superposed to the reference

in closed-loop is to find the best plant model which minimizes the prediction error between the measured output of the true closed-loop system and the predicted closed-loop output. The use of these methods requires the knowledge of the controller.

As it can be seen from Fig. 8.2, the minimization of the closed-loop prediction error will minimize the difference between real and estimated sensitivity functions. For the case of the excitation added to the controller output, the difference between

$$S_{yv} = \frac{q^{-d}BS}{AS + q^{-d}BR} \tag{8.1}$$

and

$$\hat{S}_{yv} = \frac{q^{-d}\hat{B}S}{\hat{A}S + q^{-d}\hat{B}R} \tag{8.2}$$

will be minimized, where $\hat{A}$ and $\hat{B}$ are the estimates of the A and B polynomials.[1]

For the case of the excitation added to the reference, with $T = R$, the difference between

$$S_{yr} = \frac{q^{-d}BR}{AS + q^{-d}BR} \tag{8.3}$$

and

$$\hat{S}_{yr} = \frac{q^{-d}\hat{B}R}{\hat{A}S + q^{-d}\hat{B}R} \tag{8.4}$$

will be minimized. Since $|S_{yr} - \hat{S}_{yr}| = |S_{yp} - \hat{S}_{yp}|$, the difference between the true and the estimated output sensitivity function will also be minimized.

In the context of active vibration control, we will be in general interested to get a model which allows a better estimation of the output sensitivity function. Therefore, often, the configuration of Fig. 8.2b will be used with $T = R$.[2]

The Algorithms

$$G(q^{-1}) = \frac{q^{-d}B(q^{-1})}{A(q^{-1})}, \tag{8.5}$$

where

$$B(q^{-1}) = b_1 q^{-1} + \cdots + b_{n_B} q^{-n_B} = q^{-1}B^*(q^{-1}) \tag{8.6}$$

$$A(q^{-1}) = 1 + a_1 q^{-1} + \cdots + a_{n_A} q^{-n_A} = 1 + q^{-1}A^*(q^{-1}) \tag{8.7}$$

The plant is operated in closed-loop with an RST digital controller (without lack of generality). The output of the plant operating in closed-loop is given by (see Fig. 8.2a):

$$y(t+1) = -A^* y(t) + B^* u(t-d) + A\eta(t+1) = \theta^T \varphi(t) + A\eta(t+1), \tag{8.8}$$

where $u(t)$ is the plant input, $y(t)$ is the plant output, $\eta(t)$ is the output noise and:

$$\theta^T = [a_1 \ldots, a_{n_A}, b_1 \ldots, b_{n_B}] \tag{8.9}$$

$$\varphi^T(t) = [-y(t) \ldots, -y(t - n_A + 1), u(t-d) \ldots, u(t - n_B + 1 - d)] \tag{8.10}$$

$$u(t) = -\frac{R}{S}y(t) + r_u, \tag{8.11}$$

where r_u is the external excitation added to the output of the controller (r_u is equal to $\frac{T}{S}r$ if the external excitation is applied on the reference as in Fig. 8.2b).

[1] In this case, S_{yv} corresponds to the transfer function between $r_u(t)$ and $y(t)$.

[2] This is equivalent to sending the excitation to the input of the filter R in Fig. 8.2b.

For a fixed value of the estimated parameters, the predictor of the closed-loop (the design system) can be expressed as:

$$\hat{y}(t+1) = -\hat{A}^*\hat{y}(t) + \hat{B}^*\hat{u}(t-d) = \hat{\theta}^T\phi(t), \tag{8.12}$$

where

$$\hat{\theta}^T = [\hat{a}_1 \ldots, \hat{a}_{n_A}, \hat{b}_1 \ldots, \hat{b}_{n_B}] \tag{8.13}$$

$$\phi^T(t) = [-\hat{y}(t) \ldots, -\hat{y}(t-n_A+1), \hat{u}(t-d) \ldots, \hat{u}(t-n_B+1-d)] \tag{8.14}$$

$$\hat{u}(t) = -\frac{R}{S}\hat{y}(t) + r_u \tag{8.15}$$

The closed-loop prediction (output) error is defined as:

$$\varepsilon_{CL}(t+1) = y(t+1) - \hat{y}(t+1) \tag{8.16}$$

It clearly results from Fig. 8.2a that for constant values of the estimated parameters, the predictor regressor vector $\phi(t)$ depends only upon the external excitation. Therefore under the assumption that the external excitation (r or r_u) and the stochastic noise η are independent, $\phi(t)$ and $\eta(t)$ are not correlated (as well as $\phi(t)$ and $\varepsilon_{CL}(t+1)$), the scheme has the structure of an output error prediction.

If known fixed parts should be included in the estimated plant model, the equation of the predictor for the closed-loop has to be modified in order to preserve the input/output behaviour. See for details Sect. 8.2.4 and [3].

For all the methods, the parameter adaptation algorithm (PAA) has the general form

$$\hat{\Theta}(t+1) = \hat{\Theta}(t) + F(t)\Phi(t)\nu(t+1) \tag{8.17}$$

$$F(t+1)^{-1} = \lambda_1(t)F(t)^{-1} + \lambda_2(t)\Phi(t)\Phi^T(t) \tag{8.18}$$

$$0 < \lambda_1(t) \leq 1\,;\, 0 \leq \lambda_2(t) < 2\,;$$

$$F(0) > 0\,;\, F(t)^{-1} > \alpha F^{-1}(0)\,;\, 0 < \alpha < \infty \tag{8.19}$$

$$F(t+1) = \frac{1}{\lambda_1(t)}\left[F(t) - \frac{F(t)\Phi(t)\Phi^T(t)F(t)}{\frac{\lambda_1(t)}{\lambda_2(t)} + \Phi^T(t)F(t)\Phi(t)}\right] \tag{8.20}$$

$$\nu(t+1) = \frac{\nu^\circ(t+1)}{1 + \Phi^T(t)F(t)\Phi(t)}, \tag{8.21}$$

where $\nu^\circ(t+1) = f_1(\hat{\Theta}(t), \hat{\Theta}(t-1), \ldots, y(t+1), \nu(t), \nu(t-1), \ldots)$ is the *a priori* adaptation error, $\nu(t+1) = f_2(\hat{\Theta}(t+1), \hat{\Theta}(t), \ldots, y(t+1), \nu(t), \nu(t-1), \ldots)$ is the *a posteriori* adaptation error and $\Phi(t)$ is the observation vector.

For each recursive identification algorithm Θ, Φ, and $\nu^\circ(t+1)$ will have specific expressions. Note that the sequences $\lambda_1(t)$ and $\lambda_2(t)$ allow to define the time profile of the adaptation gain $F(t)$. For convergence analysis in the stochastic environment,

it is assumed that a PAA with decreasing adaptation gain is used (i.e., $\lambda_1(t) \equiv 1$, $\lambda_2(t) = \lambda_2 > 0$).

The fundamental differences with respect to the open-loop output error identification algorithm come from the structure of the adjustable predictor and of the observation vector.

8.2.1 The Closed-Loop Output Error Algorithm

Replacing now the fixed predictor of the closed-loop given in (8.12) by an adjustable predictor, one gets:

- *a priori predicted output*:

$$\hat{y}^{\circ}(t+1) = \hat{y}(t+1|\hat{\theta}(t)) = \hat{\theta}^T(t)\phi(t); \tag{8.22}$$

- *a posteriori predicted output*:

$$\hat{y}(t+1) = \hat{y}(t+1|\hat{\theta}(t+1)) = \hat{\theta}^T(t+1)\phi(t); \tag{8.23}$$

- *a priori* prediction error as:

$$\varepsilon^{\circ}_{CL}(t+1) = y(t+1) - \hat{y}^{\circ}(t+1); \tag{8.24}$$

- *a posteriori* prediction error as:

$$\varepsilon_{CL}(t+1) = y(t+1) - \hat{y}(t+1). \tag{8.25}$$

The equation for the *a posteriori* prediction error becomes in the deterministic environment (no noise, see [4] for details):

$$\varepsilon_{CL}(t+1) = \frac{S}{P}[\theta - \hat{\theta}(t+1)]^T\phi(t) \tag{8.26}$$

The rules given in Chap. 4 suggest a PAA with:

$$\begin{aligned} \hat{\Theta}(t) &= \hat{\theta}(t) \\ \Phi(t) &= \phi(t) \\ \nu^{\circ}(t+1) &= \varepsilon^{\circ}_{CL}(t+1) \end{aligned}$$

This is termed the *Closed-Loop Output Error* (CLOE) algorithm [1, 2, 4]. It can be shown (see [2, 4] that in both deterministic and stochastic environment the sufficient condition for stability and unbiased asymptotic convergence is:

$$H'(z^{-1}) = \frac{S(z^{-1})}{P(z^{-1})} - \frac{\lambda_2}{2} \tag{8.27}$$

should be strictly positive real (where $\max_t \lambda_2(t) \leq \lambda_2 < 2$).

To relax this condition, the following two solutions have been proposed.

8.2.2 *Filtered and Adaptive Filtered Closed-Loop Output Error Algorithms (F-CLOE, AF-CLOE)*

Equation (8.26) for $\hat{\theta} = constant$ can also be rewritten as:

$$\varepsilon_{CL}(t+1) = \frac{S}{P} \cdot \frac{\hat{P}}{S}[\theta - \hat{\theta}]\frac{S}{\hat{P}}\phi(t) = \frac{\hat{P}}{P}[\theta - \hat{\theta}]\phi_f(t), \tag{8.28}$$

where

$$\phi_f(t) = \frac{S}{\hat{P}}\phi(t) \tag{8.29}$$

$$\hat{P} = \hat{A}S + q^{-d}\hat{B}R \tag{8.30}$$

In Eq. (8.30), $\hat{P}$ is an estimation of the true closed-loop poles based on an initial estimation of the plant model (for example using an open-loop experiment). This formulation leads to the *Filtered Closed-Loop Output Error* (F-CLOE) algorithm [2] which uses the same adjustable predictor as CLOE (see Eqs. (8.22) and (8.23)) and the PAA with:

$$\begin{aligned} \hat{\Theta}(t) &= \hat{\theta}(t) \\ \Phi(t) &= \phi_f(t) \\ \nu^\circ(t+1) &= \varepsilon^\circ_{CL}(t+1) \end{aligned}$$

It can be shown that by neglecting the non-commutativity of time-varying operators (an exact algorithm can however be derived), under the sufficient condition that:

$$H'(z^{-1}) = \frac{\hat{P}(z^{-1})}{P(z^{-1})} - \frac{\lambda_2}{2} \tag{8.31}$$

is strictly positive real, both asymptotic stabilities in deterministic environment and asymptotic unbiasedness in a stochastic environment are assured [2].

One can further relax the condition of Eq. (8.31) by filtering $\phi(t)$ through a time-varying filter $S/\hat{P}(t)$, where $\hat{P}(t)$ corresponds to the current estimate of the closed-loop given by: $\hat{P}(t) = \hat{A}(t)S + q^{-d}\hat{B}(t)R$, where $\hat{A}(t)$ and $\hat{B}(t)$ are the current estimates of the A and B polynomials (the AF-CLOE algorithm).

8.2.3 Extended Closed-Loop Output Error Algorithm (X-CLOE)

For the case where the noise model is $\eta(t+1) = \frac{C}{A}e(t+1)$, where $e(t+1)$ is a zero mean gaussian white noise and $C(q^{-1}) = 1 + q^{-1}C^*(q^{-1})$ is an asymptotically stable polynomial, an extended output error prediction model can be defined:

$$\begin{aligned}\hat{y}(t+1) &= -\hat{A}^*\hat{y}(t) + \hat{B}^*\hat{u}(t-d) + \hat{H}^*\frac{\varepsilon_{CL}(t)}{S} \\ &= \hat{\theta}^T\phi(t) + \hat{H}^*\frac{\varepsilon_{CL}(t)}{S} = \hat{\theta}_e^T\phi_e(t) \end{aligned} \tag{8.32}$$

Equation (8.8) for the plant output becomes in this case:

$$y(t+1) = \theta^T\phi(t) + H^*\frac{\varepsilon_{CL}(t)}{S} - C^*\varepsilon_{CL}(t) + Ce(t+1) \tag{8.33}$$

$$= \theta_e^T\phi_e(t) - C^*\varepsilon_{CL}(t) + Ce(t+1), \tag{8.34}$$

where

$$H^* = h_1 + h_2q^{-1} + \cdots + h_{n_H}q^{-n_H+1} = C^*S - A^*S - q^{-d}B^*R, \tag{8.35}$$

$$H = 1 + q^{-1}H^* = 1 + CS - P, \tag{8.36}$$

$$\theta_e^T = [\theta^T, h_1, \ldots, h_{n_H}], \tag{8.37}$$

$$\hat{\theta}_e^T = [\hat{\theta}^T, \hat{h}_1, \ldots, \hat{h}_{n_H}], \tag{8.38}$$

$$\phi_e^T(t) = [\phi^T(t), \varepsilon_{CLf}(t), \ldots, \varepsilon_{CLf}(t-n_H+1)], \tag{8.39}$$

$$\varepsilon_{CLf}(t) = \frac{1}{S}\varepsilon_{CL}(t). \tag{8.40}$$

Subtracting (8.32) from (8.34), one obtains the following expression for the closed-loop prediction error (for details see [5]):

$$\varepsilon_{CL}(t+1) = \frac{1}{C}[\theta_e - \hat{\theta}_e]^T\phi_e(t) + e(t+1). \tag{8.41}$$

Equation (8.41) clearly shows that for $\hat{\theta}_e = \theta_e$ the closed-loop prediction error tends asymptotically towards $e(t+1)$.

Replacing the fixed predictor (8.32) with an adjustable one, a recursive identification algorithm (X-CLOE) can be obtained by using a PAA with:

$$\begin{aligned}\hat{\Theta}(t) &= \hat{\theta}_e(t) \\ \Phi(t) &= \phi_e(t) \\ \nu^\circ(t+1) &= \varepsilon_{CL}^\circ(t+1) = y(t+1) - \hat{\theta}_e^T(t)\phi_e(t)\end{aligned}$$

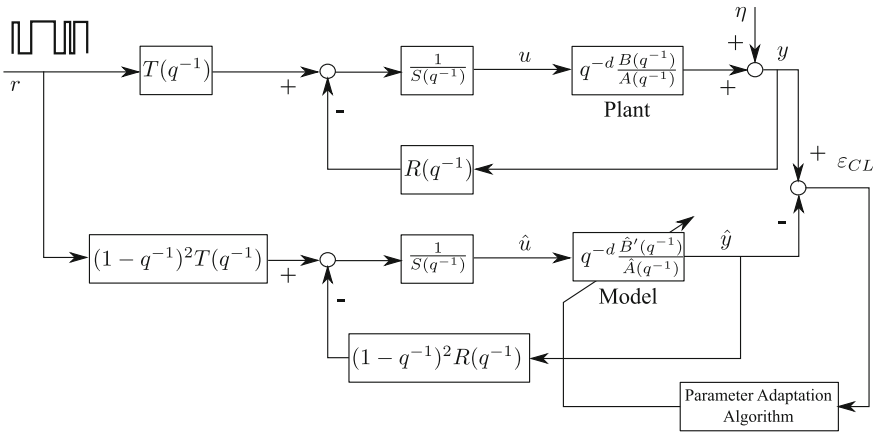

Fig. 8.3 Taking into account the double differentiator behaviour for identification in closed-loop

The analysis in the deterministic case ($C = 1, e = 0$) using the theorem given in Chap. 4 shows that global asymptotic stability is assured without any positive real condition (since the *a posteriori* closed-loop prediction error equation in this case is $\varepsilon_{CL} = [\theta_e - \hat{\theta}_e(t+1)]^T \phi_e(t)$).

Asymptotic unbiased estimates in a stochastic environment can be obtained under the sufficient condition [2, 5] that:

$$H'(z^{-1}) = \frac{1}{C(z^{-1})} - \frac{\lambda_2}{2} \tag{8.42}$$

is strictly positive real (where $\max_t \lambda_2(t) \leq \lambda_2 < 2$).

8.2.4 *Taking into Account Known Fixed Parts in the Model*

In the context of active vibration control systems, like for identification in open-loop operation, it is wise to take into account that the secondary path has a known double differentiator behaviour. This will require a modification of the controller used in the closed-loop predictor. To take into account the double differentiator behaviour when external excitation is superposed to the input of the controller (at the input of the filter R) one should modify the CLOE configuration as shown in Fig. 8.3.[3]

[3]The external excitation effect is equivalently obtained by filtering the signal through R and adding it to the output of the filter R in the upper part of the Fig. 8.3. Using algorithms from the CLID toolbox, both T and R should be modified according to the Fig. 8.3.

8.2.5 Properties of the Estimated Model

It is very important to asses the properties of the estimated model in the frequency domain. This will allow to know in what frequency region the approximation of the true plant will be best (it is expected that this should be particularly true in the critical regions for design). Nevertheless, the properties of the estimated models will depend on the point where the external excitation is applied. There are several options. When the excitation is superposed to the output of the controller (like in Fig. 8.2a), the properties of the estimated model in the frequency domain (bias distribution) result from ([2]):

$$\hat{\theta}^* = \arg\min_{\hat{\theta}\in\mathscr{D}} \int_{-\pi}^{\pi} |S_{yp}|^2 [|G - \hat{G}|^2 |\hat{S}_{yp}|^2 \phi_{r_u}(\omega) + \phi_\eta(\omega)] \mathrm{d}\omega, \tag{8.43}$$

where $\phi_{r_u}(\omega)$ and $\phi_\eta(\omega)$ are the power spectral densities of the excitation and the measurement noise, respectively. This expression shows that

- The estimation of the plant model parameters is unbiased when G is in the model set[4];
- The bias distribution is not affected by the spectrum of the noise (which is the case when using the (filtered) open-loop identification methods [2]);
- The approximation of the true model is not only weighted by the sensitivity function but is further weighted by the estimated output sensitivity function; and
- Quality of the estimated model is enhanced in the critical region for design.[5]

By contrast the bias distribution in the frequency domain for the open-loop output error is given by:

$$\hat{\theta}^* = \arg\min_{\hat{\theta}\in\mathscr{D}} \int_{-\pi}^{\pi} [|G - \hat{G}|^2 |\phi_{r_u}(\omega) + \phi_\eta(\omega)] \mathrm{d}\omega \tag{8.44}$$

As one can see, the basic difference is that in open-loop identification using output error algorithm one has an equal weight for all the frequencies. The comparison between (8.43) and (8.44), explains why identification in closed-loop may provide better models for design.

When the external excitation signal is superposed to the input of the controller, with $T = R$, the asymptotic bias distribution is given by:

$$\hat{\theta}^* = \arg\min_{\hat{\theta}\in\mathscr{D}} \int_{-\pi}^{\pi} |S_{yp}|^2 [|G - \hat{G}|^2 |\hat{S}_{up}|^2 \phi_{r_u}(\omega) + \phi_\eta(\omega)] \mathrm{d}\omega, \tag{8.45}$$

[4] Both true plant model and estimated plant model have the same orders.

[5] Recall that the maximum of the output sensitivity function corresponds to the minimum distance with respect to the Nyquist point.

where $\hat{S}_{up} = -\hat{A}R/\hat{P}$ is the estimated input sensitivity function.

For more details see [2, 6].

8.2.6 *Validation of Models Identified in Closed-Loop Operation*

As in open-loop identification, it is the model validation that will tell us on one hand if the identified model is acceptable and on the other hand it will allow us to select the best model among the models provided by various identification methods.

The objective of the model validation in closed-loop operation is to find what plant model combined with the current controller provides the best prediction of the behaviour of the closed-loop system. The results of model validation in closed-loop will depend upon the controller used.

Four validation procedures can be defined:

1. Statistical validation tests on the closed-loop output error (uncorrelation test between $\varepsilon_{CL}(t+1)$ and $\hat{y}(t)$).
2. Closeness of the computed and identified poles of the closed-loop system.
3. Closeness of the computed and identified sensitivity functions of the closed-loop system.
4. Time response validation (comparison of time responses of the real closed-loop system and of the closed-loop predictor).

Statistical Validation

The statistical validation follows the same principles as for open-loop model identification; however, in this case one considers the residual prediction error between the output of the plant operating in closed-loop and the output of the closed-loop predictor. An uncorrelation test will be used.

Using the schemes shown in Fig. 8.2b (or Fig. 8.3), where the predictor is given by Eq. (8.12) through (8.15), one computes with the identified values of the parameters:

- The cross correlations between the residual closed-loop output error $\varepsilon_{CL}(t+1)$ and the predicted output $\hat{y}(t)$);
- The covariance of the residual closed-loop output error.

This type of test is motivated on one hand by the fact that uncorrelation between the predicted output and the residual closed-loop prediction error leads to unbiased parameter estimates and on the other hand this uncorrelation implies the uncorrelation between the closed-loop output error and the external excitation. This means that the residual prediction error does not contain any information which depends upon the external excitation and therefore all the correlations between the external excitation and the output of the closed-loop system are captured by the closed-loop predictor.

One computes:

$$R_\varepsilon(0) = \frac{1}{N}\sum_{t=1}^{N} \varepsilon_{CL}^2(t) \tag{8.46}$$

$$R_{\hat{y}}(0) = \frac{1}{N}\sum_{t=1}^{N} \hat{y}^2(t) \tag{8.47}$$

$$R_{\varepsilon\hat{y}}(i) = \frac{1}{N}\sum_{t=1}^{N} \varepsilon_{CL}(t)\hat{y}(t-i) \qquad i = 1, 2, \ldots, n_A \tag{8.48}$$

$$RN_{\varepsilon\hat{y}}(i) = \frac{R_{\varepsilon\hat{y}}(i)}{[R_{\hat{y}}(0) \cdot R_\varepsilon(0)]^{1/2}} \tag{8.49}$$

As a confidence test, one can use the criterion

$$|RN(i)| \leq \frac{2.17}{\sqrt{N}}, \tag{8.50}$$

where N is the number of data (see also Sect. 5.5), as well as the practical criterion $|RN(i)| \leq 0.15$.

In many practical situations, one either has a previous plant model identified in open-loop or several identification algorithms are used on the data collected in closed-loop. Then a comparative validation has to be done and useful comparison indicators are provided by $R_\varepsilon(0)$ and $\max |RN_{\varepsilon\hat{y}}|$ for each model (however other comparison criteria can be considered).

Pole Closeness Validation

If the model identified in closed-loop in feedback with the controller used during identification allows constructing a good predictor for the real system, this implies that the poles of the closed-loop system and of the closed-loop predictor are close (assuming that a persistent excitation has been applied for identification). As a consequence, the closeness of the closed-loop predictor poles (which can be computed) and those of the real closed-loop system (which can be identified by an open-loop type identification between the external excitation and the output) will give an indication of the quality of the identified model.

The closeness of the two sets of poles can be judged by a visual examination of the poles chart but a quantification of the closeness can be done (see next).

Sensitivity Functions Closeness Validation

From the same arguments as above it results that if the identified model is good, the sensitivity functions of the closed-loop predictor (which can be computed) are close to the sensitivity functions of the real system (which can be identified by an open-loop type identification between the external excitation and the output).

To some extent the closeness of the sensitivity functions can be assessed by visual inspection. Moreover it is possible to quantify rigorously the distance between two transfer functions by computing the Vinnicombe distance (see Appendix A).

Extensive simulations and a large number of experimental results have shown that the statistical tests and the poles or sensitivity functions closeness give coherent results and allow a clear comparison between several models ([1]).

Time Domain Validation

For the validation in the time domain, the time responses of the closed-loop system and of the closed-loop predictor are compared. Unfortunately in practice it is in general not easy to compare accurately several models using this technique. In fact a good validation by poles or sensitivity functions closeness will imply a good superposition of the time domain responses while the reciprocal is not always true.

8.3 A Real-Time Example: Identification in Closed-Loop and Controller Redesign for the Active Control System Using an Inertial Actuator

A first controller for this system has been designed in Sect. 7.3 using a plant model identified in open-loop and it has been tested in real time. The objective in this section is to illustrate the procedure for identification in closed-loop operation. For carrying the identification in closed-loop operation the controller designed on the basis of the open-loop identified model will be used. The identification experiment is done in the absence of the narrow-band output disturbance.

In this example the objective of the identification in closed-loop will be to heavily weight the differences between the estimated model and the true model in the frequency regions close to the Nyquist point. This is achieved by adding the excitation signal to the control signal (see Sect. 8.2.5).

To take into account the double differentiator behaviour of the secondary path model, the solution indicated in Fig. 8.3 has been used, i.e., the double differentiator has been added to the polynomials $T(q^{-1}) = S(q^{-1})$ and $R(q^{-1})$.

Before running the identification algorithms, the input and output signals have been centred. The orders of the model used for identification in closed-loop operation are the same as those of the model identified in open-loop ($n_B = 23$ and $n_A = 22$). The final order for the secondary path numerator after adding the known fixed part will be $n_B = 25$.

A parameter adaptation algorithm with decreasing gain has been used for all the identification methods. The best results in terms of validation have been obtained using the X-CLOE method. The uncorrelation validation test result for the closed-loop identification is shown in Fig. 8.4. It can be seen that the model is valid. The loss function is 7.7×10^{-5} an it is very small compared to the measured output.

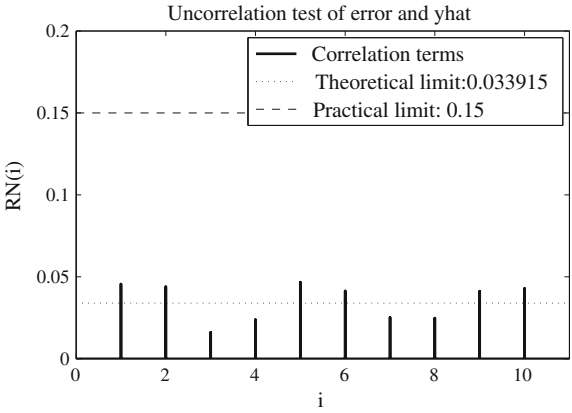

Fig. 8.4 Uncorrelation test for the model identified in closed-loop operation with XCLOE

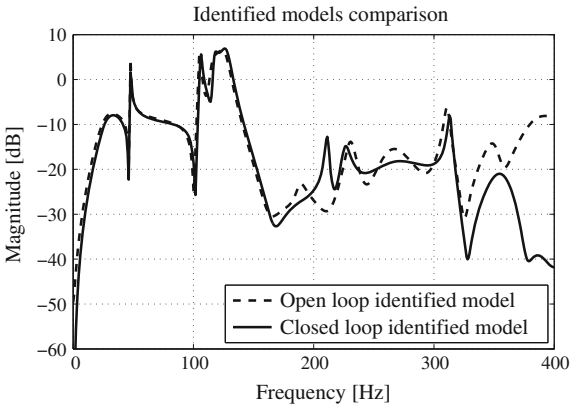

Fig. 8.5 Comparison between the frequency characteristics of the secondary path models identified in open-loop and in closed-loop operation

A comparison with an open-loop identification of the closed-loop has also been accomplished to validate the model. The open-loop model does not pass the uncorrelation test on the closed-loop data; the loss function for the open-loop identified model on the closed-loop data is 1.3×10^{-3} (much higher than for the model identified in closed-loop). One can conclude already that the model identified in closed-loop operation is better than the model identified in open-loop operation. A Bode magnitude comparison between the open-loop identified model from Sect. 6.2 and the closed-loop identified model in the presence of the controller designed in Sect. 7.3 is shown in Fig. 8.5. It can be observed that the two models are very close in the frequency region of interest (50–95 Hz). Note that the differences between the two transfer functions appear in the frequency region over 150 Hz, where the magnitude of the input sensitivity function is very low (see Fig. 7.14) and therefore there will be a little impact on performances.

Further comparison between the two models requires an estimation of the closed-loop transfer function. The closed-loop between excitation and measurement has

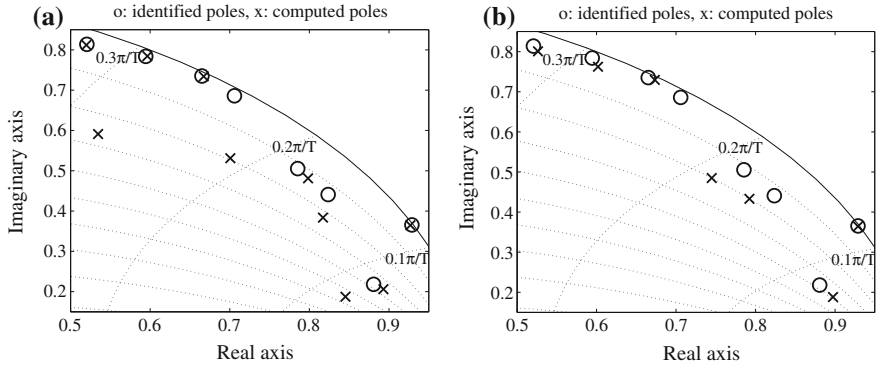

Fig. 8.6 Closed-loop poles closeness comparison using the model identified in closed-loop operation (**a**) and the open-loop identified model (**b**)

been identified as an input/output model using XOLOE method. The identified model of the closed-loop passed the whiteness test (i.e., it is a valid model). This allows to compare the identified closed-loop poles with the calculated closed-loop poles using the two models identified in open and in closed-loop operation. The pole closeness between the poles of the identified closed-loop model and the poles computed with the open-loop identified model and with the model identified in closed-loop are shown in Fig. 8.6. The model identified in closed-loop gives a slightly better result.

Using the same specifications and controller design steps as described in Sect. 7.3, a new controller has been obtained on the basis of the model identified in closed-loop operation. The controller has been tested using the same procedure as before. Time domain results in open-loop and in closed-loop are shown in Fig. 8.7. Frequency

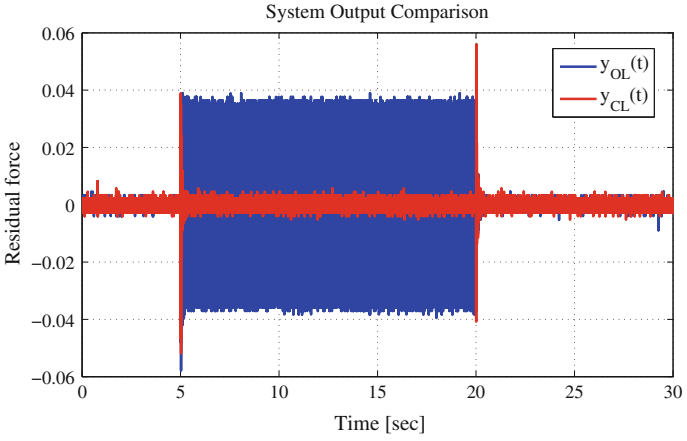

Fig. 8.7 The response results for a 70 Hz disturbance in open-loop and in closed-loop with the redesigned controller

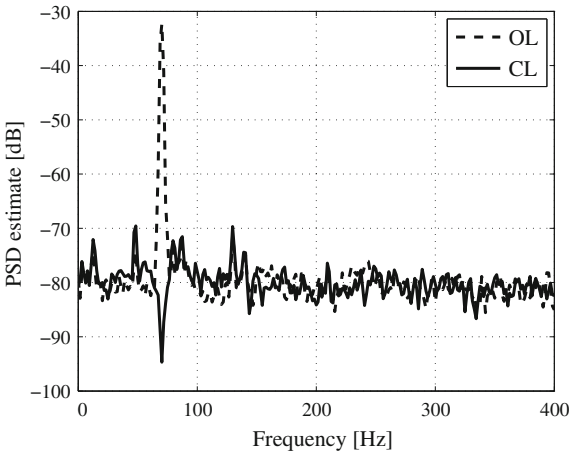

Fig. 8.8 PSD of the residual force in open-loop (*dashed line*) and closed-loop (*solid line*) for 70 Hz disturbance using the redesigned controller

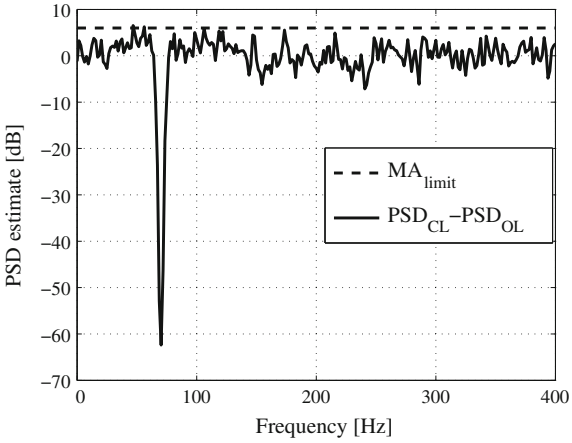

Fig. 8.9 Effective residual attenuation/amplification PSD estimates computed as the difference between the open-loop PSD and the closed-loop PSD using the redesigned controller

domain analysis has also been done and the results are shown in Figs. 8.8 and 8.9. It can be seen that the controller effectively reduces the disturbance and the residual force is at the level of the system's noise. These figures have to be compared with Figs. 7.15, 7.16, and 7.17.

The global attenuation of the newly designed controller is 49 dB, while for the first controller it was 48.4 dB. As for the first controller, the maximum amplification does not exceed the 6 dB limit (dashed line in Figs. 7.17 and 8.9). The disturbance attenuation is of 62.4 dB for the new controller and 63 dB for the initial one. The differences are negligible taking also into account that they were obtained on the basis of a single trial (one realization of a stochastic process).[6] One can conclude that in this particularvadjust case, already the quality of the model identified in open-

[6]It was not possible to conduct a sufficiently large number of measurements for this example.

loop was sufficient to get a good controller. Therefore, the initial controller based on the open-loop identified model will be used in Sect. 9.4 to design a reduced order controller.

8.4 Concluding Remarks

- Plant model identification in closed-loop operation provides efficient tools either for improving open-loop identified models or for redesign and retuning of existing controllers.
- The objective of identification in closed-loop operation is to obtain, for a given controller, a plant model allowing the best description of the behaviour of the closed-loop system.
- Identification in closed-loop is based on the use of an adaptive predictor for the closed-loop which is re-parameterized in terms of the plant model to be identified.
- The estimated parameters minimize asymptotically a criterion in terms of the closed-loop prediction error.
- As for the case of identification in open-loop, there is no single algorithm which gives the best results in all the situations.
- Comparative validation of the identified models is crucial for the selection of the best identified model.
- In addition to the statistical validation test, the pole closeness between the true closed-loop poles (obtained through identification of the closed-loop) and the computed ones, based on the identified model is a very useful validation tool.

8.5 Notes and References

Plant model identification in closed-loop operation has been considered for a long time as a very difficult problem. See [7] for a survey.

It is the work done on the topics of "Identification for Control" and "Iterative Identification and Controller Re-design" which contributed to put the problem of identification in closed-loop operation in an appropriate context. See [8–13] for details.

The original reference for the closed-loop output error is [4]. Further details and comparative evaluations can be found in [1, 2, 6, 14].

References

1. Landau I, Karimi A (1997) Recursive algorithms for identification in closed loop. A unified approach and evaluation. Automatica 33(8):1499–1523
2. Landau ID, Lozano R, M'Saad M, Karimi A (2011) Adaptive control, 2nd edn. Springer, London
3. Landau I, Zito G (2005) Digital control systems - Design, identification and implementation. Springer, London
4. Landau ID, Karimi A (1997) An output error recursive algorithm for unbiased identification in closed loop. Automatica 33(5):933–938. doi:10.1016/S0005-1098(96)00223-3
5. Landau ID, Karimi A (1996) An extended output error recursive algorithm for identification in closed loop. In: Proceedings of the 35th IEEE conference on decision and control, vol 2, pp 1405–1410. doi:10.1109/CDC.1996.572708
6. Karimi A, Landau I (1998) Comparison of the closed loop identification methods in terms of the bias distribution. Syst Control Lett 4:159–167
7. Soderstrom T, Stoica P (1989) System identification. Prentice Hall, New York
8. Gevers M (1993) Towards a joint design of identification and control. In: Trentelman HL, Willems JC (eds) Essays on control: perspectives in the theory and its applications. Birkhäuser, Boston, pp 111–152
9. Gevers, M (1995) Identification for control. In: Prepr. IFAC Symposium ACASP 95. Budapest, Hungary
10. Van den Hof P, Schrama R (1993) An indirect method for transfer function estimation from closed loop data. Automatica 29(6):1751–1770
11. Van den Hof P, Schrama R (1995) Identification and control—closed-loop issues. Automatica 31(12):1751–1770
12. Zang Z, Bitmead RR, Gevers M (1991) Iterative weighted model refinement and control robustness enhancement. In: Proceedings of the 30th IEEE-CDC. Brighton, UK
13. Zang Z, Bitmead RR, Gevers M (1995) Iterative weighted least-squares identification and weighted LQG control design. Automatica 31(11):1577–1594
14. Landau ID, Karimi A (1999) A recursive algorithm for ARMAX model identification in closed loop. IEEE Trans Autom Control 44(4):840–843